Articles

Crest: Centre for Research in Engineering
Surface Technology

2013

Novel Microwave Assisted Synthesis of ZnS Nanomaterials

Suresh Pillai
Technological University Dublin, suresh.pillai@tudublin.ie

Michael Seery
Technological University Dublin, michael.seery@tudublin.ie

Damian Synnott
Technological University Dublin

John Colreavy
Technological University Dublin

Stephen Hinder
Univerity of Surrey

Follow this and additional works at: https://arrow.tudublin.ie/cenresart

Part of the Chemical Engineering Commons, Environmental Chemistry Commons, Inorganic Chemistry Commons, and the Materials Chemistry Commons

Recommended Citation

Novel Microwave Assisted Synthesis of ZnS Nanomaterials

Damian W Synnott,[1,2] Michael K Seery,[2] Steven J Hinder,[3] John Colreavy[1] and Suresh C Pillai.[1,*]

[1] Centre for Research in Engineering Surface Technology, Dublin Institute of Technology, FOCAS Institute, Camden Row, Dublin 8 (Ireland) E-mail: suresh.pillai@dit.ie

[2] School of Chemical and Pharmaceutical Sciences, Dublin Institute of Technology, Kevin St., Dublin 8 (Ireland)

[3] School of Engineering, University of Surrey, Guildford, Surrey, GU2 7XH (United Kingdom)

Abstract

A novel ambient pressure microwave-assisted technique is developed in which silver and indium modified ZnS is synthesised. The as prepared ZnS is characterised by X-ray diffraction, UV-Vis spectroscopy, X-ray photoelectron spectroscopy and luminescence spectroscopy. This procedure produced crystalline materials with particle sizes below 10 nm. The synthesis technique leads to defects in the crystal which induce mid energy levels in the band gap and lead to indoor light photocatalytic activity. Increasing the amount of silver causes a phase transition from cubic blende to hexagonal phase ZnS. In a comparative study, when the ZnS cubic blende is heated in a conventional chamber furnace, it is completely converted to ZnO at 600 °C. Both cubic blende and hexagonal ZnS show excellent photocatalytic activity under irradiation from a 60 watt light bulb. These ZnS samples also show significantly higher photocatalytic activity compared to the commercially available TiO_2 (Evonik-Degussa P-25).

1. Introduction

Zinc sulfide, a type II-VI semiconductor material, has been extensively studied due to its unique optical properties, luminescent properties and catalytic activity.[1,2,3,4,5] ZnS exists in two structural polymorphs, cubic blende sphalerite and hexagonal wurtzite. Of the two polymorphs, the cubic blende is considered as the stable phase at standard temperature and pressure. Cubic blende ZnS has a face centered cubic structure in which both the zinc and sulfur atoms are tetrahedrally coordinated. Wurtzite phase ZnS is more thermodynamically stable at temperatures above 1020 °C, but can exist as a metastable phase at standard temperature and pressure. The wurtzite phase has a hexagonal close packed structure in which the Zn and S atoms are also tetrahedrally coordinated. In nanosized materials, many factors can change the phase transition temperature, including the small size, increased pressure, surface modification, and precipitation rates during the synthesis of the semiconductor.[6,7,8,9,10,11,12]

A low temperature preparation of hexagonal ZnS is desirable because the prepared wurtzite nanostructures can meet thermal stability required for reliable optoelectronic device operation, including the incorporation of these materials in flexible substrates such as plastics. The hexagonal structure is also the more desirable structure for its optical properties than the cubic blende structure.[6-12] Cubic blende ZnS has been synthesized in a number of ways including by precipitation, by hydrothermal synthesis, and using ultrasonic irradiation.[13,14,15] Using these techniques for large scale synthesis limits the applications of ZnS as a photocatalyst due to the high cost, difficulty in separation, recovery and recycling in industrial environments. Some of these reactions also require high temperatures and the use of H_2S as a starting material. Microwave synthesis has gained a lot of

attention in recent times for the preparation of organic compounds, molecular sieves and radiopharmaceuticals, and also for the fabrication of zeolites and inorganic materials. Compared to conventional techniques, the use of microwave has advantages of quick reaction times, rapid volumetric heating, small particle size, low cost and energy saving.[16,17,18]

2. Experimental

2.1 Preparation of Nanomaterials

Powdered nanoparticles were prepared by a microwave assisted irradiation methodology. In a typical synthesis, an aqueous zinc acetate dihydrate solution (200 mL, 0.2 M) was added to an aqueous solution of thiourea (200 mL, 0.2 M). To this indium acetate (4 mL, 0.04 M) and silver nitrate (10 mL, 0.04 M) were added. The open beaker containing these solutions was placed in a MARS 5 industrial microwave system and was irradiated at 600 W for 30 min followed by a 5 min cool down period. After the time had elapsed the water had completely evaporated and dry yellowish brown powder was collected and characterized without further treatment. This produced a 1 % Ag – 0.4 % In ZnS sample.

2.2 Characterisation

The obtained ZnS was investigated using a combination of characterisation techniques including X-ray diffraction using a Siemens D 500 X-ray diffractometer with the diffraction angles scanning from $2\theta = 20 - 80$ °, using a Cu Kα radiation source. The diffuse absorbance spectra of the samples were measured by a UV-Vis-NIR Perkin Elmer 900 spectrometer between 800 and 200 nm, using a black KBr disc as a reference. Luminescence measurements were taken, with samples suspended in ethanol, by a Perkin Elmer LS 55 luminescence spectrometer. X-ray photoelectron spectrometer measurements were taken with a Thermo VG Scientific (East Grinstead, UK) Sigma Probe spectrometer using a monochromated Al Kα X-ray source (hν = 1486.6 eV), which was used at 140 W and the area of analysis was approximately 500 µm in diameter. Scanning electron microscopy images were obtained using a Hitachi SU-70 FE-SEM.

2.3 Photocatalysis Testing

Photocatalysis testing was carried out using methylene blue as a model pollutant and a 60 W bulb as a light source to simulate indoor lighting conditions. In a standard test, 60 mg of photocatalyst powder was added to methylene blue (50 mL, 1 x 10^{-5} M) and the powder and solution was stirred for 30 m in the dark, to allow for any adsorption of the dye onto the particle to occur. Then the dye and photocatalyst were irradiated for 2 h with samples taken every 30 m. The samples were centrifuged before the absorbance of the dye was measured by UV – Vis analysis.

The degradation of the methylene blue was measured using a pseudo – first order kinetic plot where a plot of Ln(A/Ao) v time revealed the degradation rate, k.

3. Results and Discussion

The crystal structure of the as prepared powders was investigated by X-ray diffraction with Cu Kα radiation. As shown in Figure 1, the zinc sulfide prepared without silver and the samples with up to 2

mol % silver crystallize as the cubic blende form of ZnS with peaks at 28.55°, 47.55° and 56.3° corresponding to the (111), (200) and (220) planes respectively. When the mol % of silver is increased to 4 and 8 % the peaks at 27.15°, 28.75°, 30.7°, 47.7°, 51.75° and 56.45° are observed which correspond to the (100), (002), (101), (102), (110), (103) and (112) planes respectively and indicate that the wurtzite phase of ZnS is present. In the XRD patterns no peaks that show the presence of AgS or $AgInS_2$ are observed, which suggests that the silver and indium ions are added into the lattice or on the surface of the ZnS crystal rather than a solid-solution of $(AgIn)xZn_{2(1-x)}S_2$ being formed.[19] The particle size is estimated from the X-ray diffraction patterns using the Scherrer equation,[6] by measuring the line broadening of the (111) peak in cubic blende ZnS and the (002) peak for the wurtzite ZnS. For all samples up to 4 mol % silver the particle size is found to be 4 nm ± 1 and at 8 mol % silver the particle size increases to 8 nm. The broadening of the peaks suggests that the particles are nanosized. The small particle size is consistent with literature reports of ZnS prepared via microwave synthesis.7
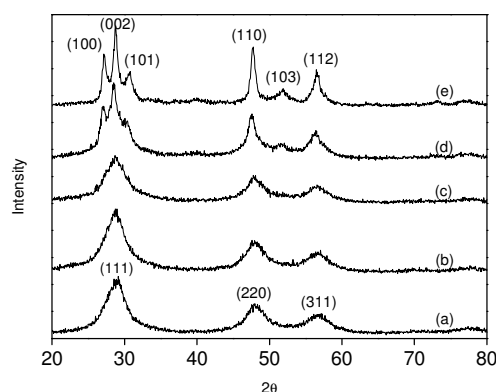

Figure 1. X-ray diffraction patterns of (a) ZnS (b) 1% Ag - 0.4 % In – ZnS (c) 2% Ag – 0.4% – ZnS (d) 4% Ag – 0.4% In – ZnS and (e) 8% Ag – 0.4% In – ZnS

Raman spectrocsopy was employed to further confirm the phase change from cubic blende to wurtzite with increased silver. Figure 2 (a) shows the raman spectrum of 0.4 % Ag – 0.4 % In ZnS which is cubic blende in phase. The peaks at 345, 546 and 700 cm^{-1} match those associated with the LO, 2TO and 2LO modes of cubic blende zinc sulfide. The peak at 261 cm^{-1} has previously been identified as a surface phonon mode. The expected peak for the TO mode at 285 cm^{-1} is absent in this case, under visible excitation (660 nm), due to poor scattering efficiency and the anti-resonant behaviour reported for the mode in cubic blende ZnS. Figure 2 (b) shows the raman spectrum for the hexagonal phase 4% Ag 0.4 % In ZnS. The peaks for cubic blende ZnS disappear for the 4 % Ag – 0.4 % In ZnS and peaks appear at 334 cm^{-1} and 532 cm^{-1}. The peak at 334 cm^{-1} has been assigned to the surface optical, SO, mode in wurtzite ZnS.[20,21,22,23,24,25]
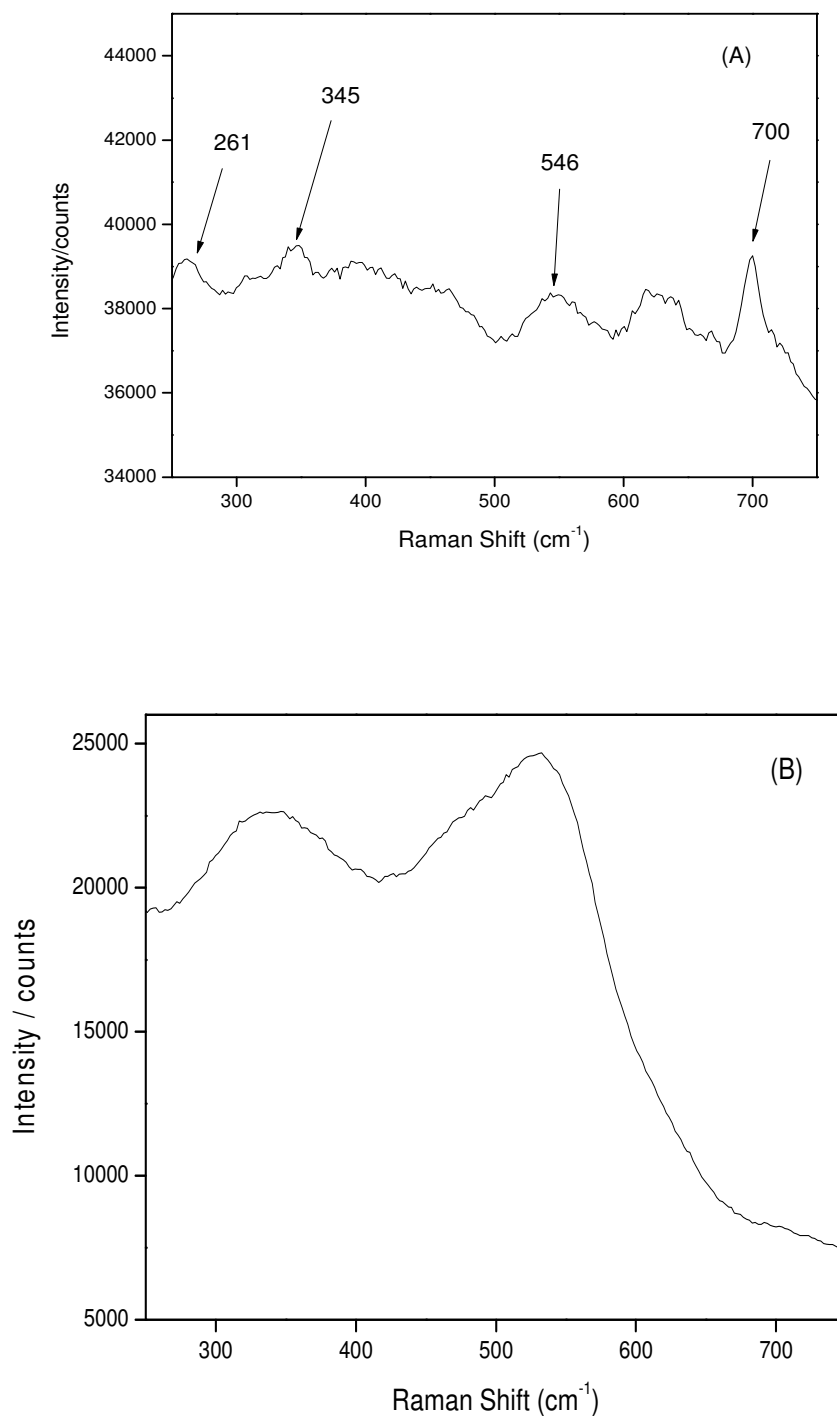
Figure 2. Raman spectra of (a) 0.4% Ag – ZnS (b) 2% Ag – ZnS

The XPS spectra (Figure 3.) of 4 % Ag – 0.4 % In ZnS show peaks located at 368.5 and 374.3 eV are consistent with those of the Ag 3d peaks and the spin-orbit splitting of the 3d doublet of 5.8 eV is characteristic of metallic silver.[26,27] The other spectra show peaks located at 1045.5, 1022.5 and 162.5

eV. These peaks correspond to the binding of the Zn 2p1, Zn 2p3 and S 2p1/2 electrons respectively and indicate the presence of ZnS.
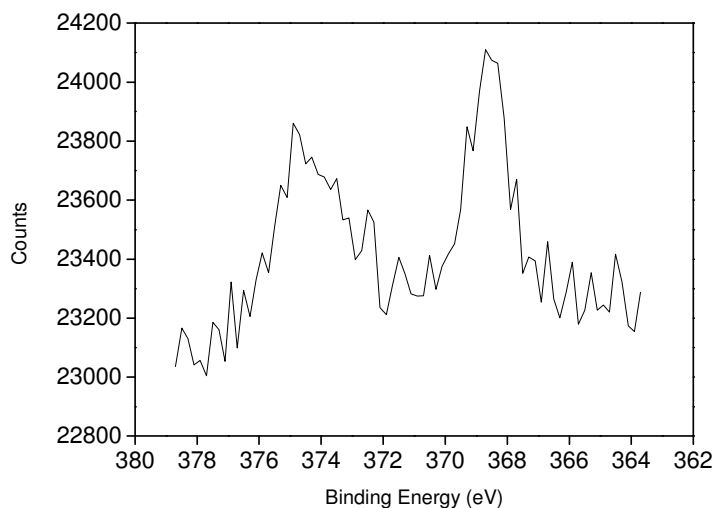

Figure 3. XPS spectra of Ag-3d for 4 % Ag – 0.4 % In ZnS

Scanning electron microscopy images (Figure 4) show a significant difference between the samples containing 0.4 % Ag and 8 % Ag. In the 0.4 % Ag-0.4 % In ZnS, the agglomerates are less than 1 µm in size with regular shapes. The 8 % Ag-0.4 % In ZnS sample shows much larger agglomerate, with irregular shapes.
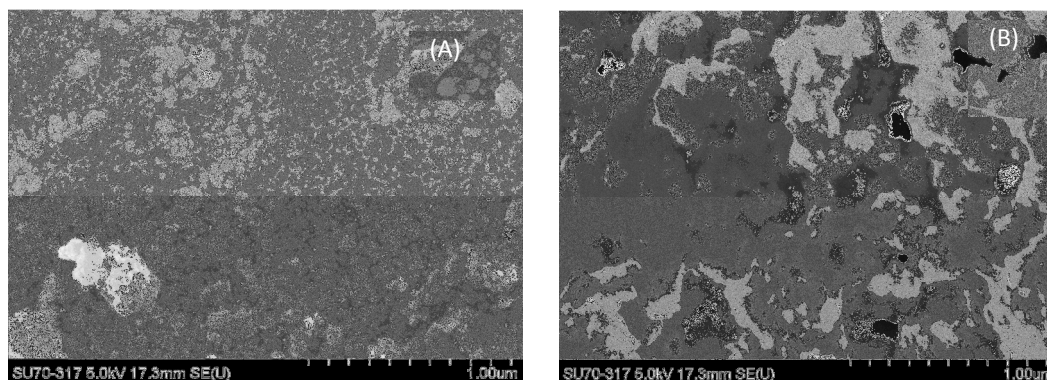

Fig 4. SEM images of (A) 0.4% Ag-0.4% In ZnS and (B) 8% Ag-0.4% In ZnS

For the samples containing up to 2 mol % silver there is an absorption edge at 319 nm (Figure 5) which equates to a band gap of 3.9 eV. This band gap is greater than that of bulk ZnS and is due to the quantum size effect owing to the nanometre size of the particles. For these samples there is an absorption shoulder that stretches to 500 nm for the 0.4 and 1 mol % silver samples and up to 570 nm for the 2 mol % silver. These shoulders show that the samples absorb light in the visible region, as supported by the yellow to orange colours of the sample. The samples containing 4 and 8 mol % silver are a brown coloured powder and the diffuse absorbance spectra show the complete absorbance up to 800 nm.
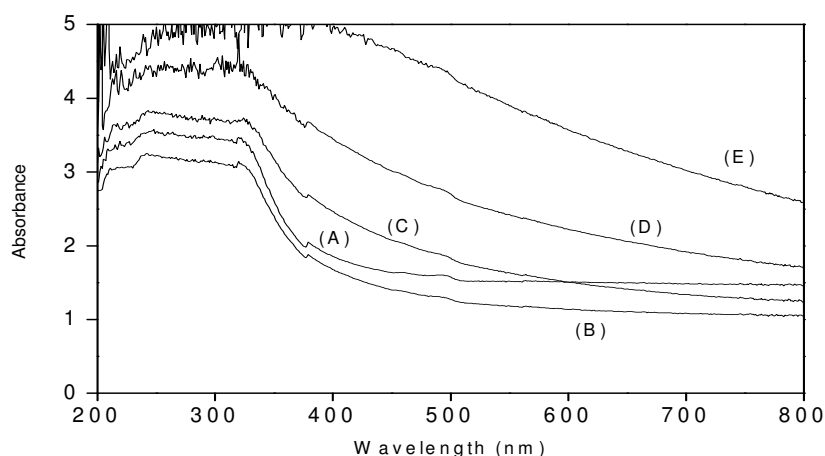
Figure 5. Diffuse absorbance spectra of (A) 0.4% Ag 0.4% In ZnS, (B) 1% Ag – 0.4 % In ZnS, (C) 2% Ag – 0.4% In ZnS, (D) 4% Ag – 0.4% In ZnS and (E) 8% Ag – 0.4% In ZnS

The luminescence spectra of the 0.4% Ag – 0.4% In ZnS sample (figure 6) show emission peaks at 385, 427 and 489 nm which correspond to three point defects within the ZnS crystal. The peak at 385 mm is related to the interstitial Zn, the peak at 427 being from S vacancies and the peak 489 nm relating to Zn vacancies. Peng *et al.*[16] showed that these defects sites act as interband donor levels and reduce the energy required to promote an electron to the conduction band and leave a hole in the valence band and thus induce photocatalysis. Conversion to hexagonal causes a 10 nm redshift in the peak associated with the interstitial Zn. This shift is due to a rearrangement of the atomic structure when the phase change occurs.
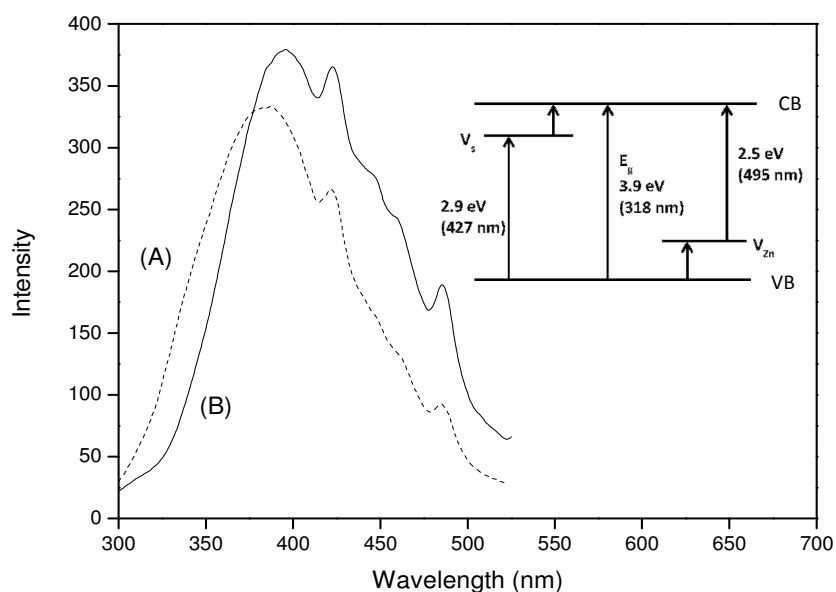
Figure 6. Emission spectra of (A) 0.4% Ag – 0.4% In ZnS and (B) 8% Ag – 0.4% In ZnS and inset is the band structure with the defects caused by zinc and sulfur vacancies

The inset of figure 6 shows the proposed energy levels of the ZnS with the vacancies of Zn and S providing steps for the electron to be promoted from the valence band to the conduction band by light of a lower energy than that of the band gap (3.9 eV). These extra energy levels within the band gap allow for excitation of the electron with visible light, with wavelengths up to 495 nm (2.5 eV).

Photocatalysis tests were carried out by measuring the degradation of a methylene blue, a model dye, in the presence of the photocatalyst under irradiation from a 60 W incandescent light bulb. The samples containing silver showed greater photocatalytic activity than the unmodified sample and Degussa P25 titanium dioxide, which is a commercially available photocatalyst. The results in Table 1 show that the sample containing 2 mol % silver had the highest photocatalytic activity while the sample containing 8 mol % silver showed no activity. The increase in activity can be attributed to the role of silver as an electron scavenger.[27,28,29] Efficient photocatalysis requires a lower recombination rate of the photo produced electrons and holes. The holes in the valence band are primarily responsible for the formation of hydroxyl radicals, which degrade the pollutant on the surface of the photocatalyst. The optimum level of silver was found to be 2 mol% in this study. Above this concentration, the photocatalytic activity begins to drop and at 8 mol % the photocatalytic activity is reduced completely. This is due to the excess silver blocks photocatalytic sites on the surface of the photocatalyst.

Table 1. Photocatalytic rates of microwave prepared ZnS and standard samples.

Sample Name	Photocatalytic Rate (min-1, x10-3)
Degussa P25 TiO_2	2.9
ZnS	5.0
0.4% Ag – 0.4% In ZnS	5.0
1% Ag – 0.4% In ZnS	6.5
2% Ag – 0.4% In ZnS	8.3
4% Ag – 0.4% In ZnS	6.1
8% Ag – 0.4% In ZnS	1.2

The role of silver is significant in phase change from cubic blende to hexagonal. It is known that the phase transition temperature can be reduced when the particles are nanosized and that the addition of addition elements also affects the transition temperature.[29] In order to understand the phase change of ZnS, the Ag-In-ZnS prepared under microwave conditions is annealed at various temperatures in a chamber furnace. When the cubic blende phase 2% Ag – 0.4% In ZnS prepared in the microwave is heated, for 2 h, at temperatures up to 600 °C, no phase transition to hexagonal ZnS occurs. At 200 and 400 °C the ZnS remains in the cubic blende phase. At 500 °C there is a mix of cubic blende ZnS and ZnO. The ZnO forms as oxidation occurs at higher temperatures. At 600 °C, the ZnS has completely transformed to ZnO. The XRD data confirming these phases is shown in Figure 7.
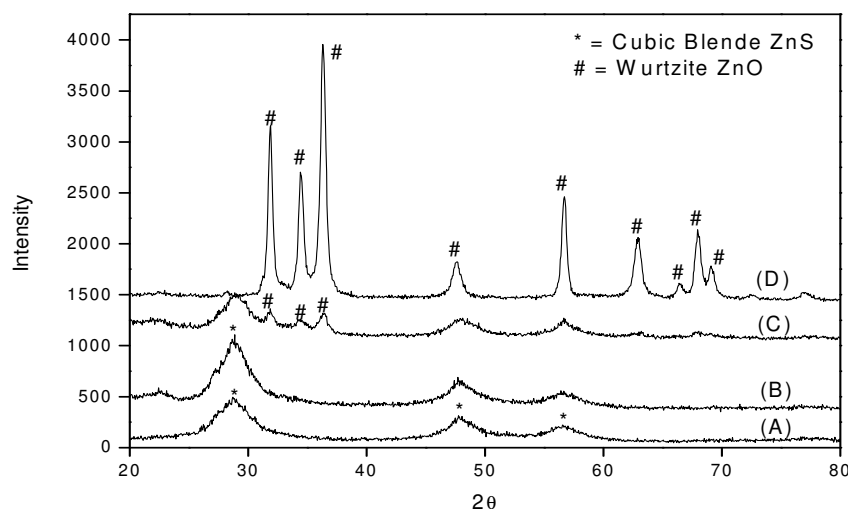
Figure 7. XRD spectra of (A) 2% Ag-0.4% In ZnS, (B) 2% Ag-0.4% In ZnS calcined at 400 °C, (C) 2% Ag - 0.4% In ZnS calcined at 500 °C and (D) 2% Ag – 0.4% In ZnS calcined at 600 °C

Under conventional synthesis methods when silver and indium are added to ZnS, mixed layer polytypes can form.[30,31] However, in the current study pure cubic blende or wurtzite ZnS is formed with different concentrations of silver added. Indium was selected as an additive to get the optimum photocatalytic properties. A preliminary study was carried out on indium modified ZnS by microwave irradiation to understand its photocatalytic activity. The level of indium was varied from 0.05 % to 2 %. From that study it was shown that ZnS with 0.4 % In addition was at the optimum level for improving the photocatalytic activity of the ZnS sample. When the Ag was introduced to the system (to study its impact on phase change), it was concluded that the level of indium should remain constant at its optimum level. The role of indium in the system from a synthetic point of view is to improve the photocatalytic activity under indoor light irradiation. The indium achieves this in two ways. The first is to provide *n* type doping by inserting a band in the semiconductor close to the valence band. This allows for electrons to be promoted to the conduction band from the indium at lower wavelengths than is required for promotion of an electron from the valence band to the conduction band. The second way in which indium improves the photocatalytic activity of the doped ZnS under indoor light irradiation is the increased number of defects in the crystal in the presence of indium. Indium incorporation into the ZnS crystal lattice can lead to an increase in faults in the crystal and in lattice distortion. This is due to the difference in the ionic radii of trivalent indium ions (0.80 Å) and the bivalent zinc ion (0.74 Å).[32] The difference in the valence of the Zn^{2+} and the In^{3+} also leads to an increase in the number of sulfur vacancies, which act as stepping stones for the electrons travelling from the conduction band to the valence band.[33] This is incorporated in the supplementary information as Table 1. The silver has two roles in the system. The first is that the metallic silver formed during the microwave irradiation affects the crystal growth of the ZnS and causes the formation of wurtzite as opposed to sphalerite which forms when only the precursors for Zn and S are involved in the reaction. The silver particles act on the surface of the crystal and affect the surface energy which leads to the transition and formation of wurtzite particles.[18] Supplementary figure 1 shows the XRD patterns for ZnS prepared with the addition of silver and no indium added. The

patterns match those of the silver and indiums co-modified material and confirm the influence of the silver on the ZnS with the hexagonal form identified when levels of silver at 4 % and above is used. (It should be noted that the composition was calculated as the molar ratio of the reagents used in the reaction. The authors acknowledge that the XPS analysis is a surface technique and is not the best method for determining composition of the bulk of the sample. It is often difficult to determine the small amount of dopants/additives using XPS or XRD. The XPS analysis shows an increasing amount of silver relative to the zinc and sulfur in a ratio that matches the recipe of the precursors). The second is the affect of the silver on the surface of the particle on the photocatalytic activity of the material. Silver particles have been shown to act as electron traps on photocatalysts. This electron trap reduces the recombination rate of the electron – hole pair and increases the photocatalytic activity.[26,34-36] Further studies are underway to understand the complete mechanism of the low temperature phase transition and look at the applications including photocatalysis and optoelectronic devices.

Conclusions

In summary, it was found that the formation of ZnS under the microwave irradiation is significantly influenced by the addition of silver and indium precursors to the precursor solutions. The addition of silver above 4 mol % causes a total phase transition from cubic blende to wurtzite ZnS. The influence of the microwave synthesis also produces a pure ZnS crystal with no silver sulfide or silver indium sulfide produced with the ZnS. The addition of silver also leads to an increase in the photocatalytic activity of the ZnS under irradiation from a 60 – watt light bulb. The silver and indium modified ZnS shows twice the photocatalytic activity compared to the commercially available TiO_2. The open beaker microwave method is shown to be a quick, straight-forward method for producing pure, photocatalytically active materials which can used without further treatment or heating.

Graphical Abstract
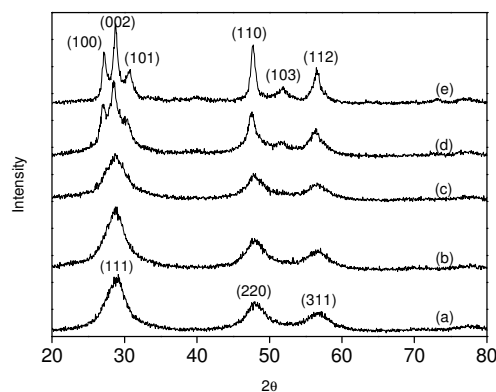
[1] Li G, Zhai J, Li D, Fang X, Jiang H, Dong Q and Wang E 2010 *J. Mater. Chem.* **20** 9215

[2] Geng J, Liu B, Hu F N and Zhu J J 2007 *Langmuir* **23** 10286

[3] Shen G Z, Bando Y, Hu J Q and Golberg D 2007 *App. Phys. Lett.* **90** 123101

[4] McClov J S, Korenstein R and Zelinski B 2009 *J. Am. Chem. Soc.* **92** 1725

[5] Chen Y C, Wang C H, Lin H Y, Li B H, Chen W T and Liu C P 2010 *Nanotechnology* **21** 455604

[6] Omurzak E, Mashimo T, Sulaimankulova S, Takebe S, Chen L, Abdullaeva Z, Iwamoto C, Oishi Y, Ihara H, Okudera H and Yoshiasa A 2011 *Nanotechnology* **22** 365602

[7] Limaye M V, Gokhale S, Acharya S A and Kalkarni S K 2008 *Nanotechnology* **19** 451602

[8] Fang X, Bando Y, Liao M, Gautam U K, Zhi C, Dierre B, Liu B, Zhai T, Sekiguchi T, koide Y and Golberg D 2009 *Adv. Mater.* **21** 2034

[9] Hu, J S, Ren L L, Guo Y G, Liang H P, Cao A M, Wan L J and Bai C I 2005 *Angew. Chem. Int. Ed.* **44** 1269

[10] Fiegal C, Russo S P and Barnard A S 2010 *J. Mater. Chem.* **20** 4971

[11] Li Y, Li C, Yang C and Li Y 2004 *J. Phys. Chem. B* **108** 16002

[12] Zhang H and Banfield J F 2009 *J. Phys. Chem. C* **113** 9681

[13] Wang Z, Daeman L L, Yusheng Z, Zha C S, Downs R T, Wang X, Wang Z L and Hemley R J 2005 *Nature Materials* **4** 922

[14] Liang Y, Liang H, Xiao X and Hark S 2012 *J. Mater. Chem.* **22** 1199

[15] Pahari S K, Sinhamahaptra A, Sutradhar N and Bajaj H C 2012 *Chem. Comm.* **48** 850

[16] Peng W Q, Cong G W, Qu S C and Wang Z G 2006 *Opt. Mater.* **29** 313

[17] Jiang C, Zhang W, Zou G, Yu W and Qian Y 2007 *Mater. Chem. Phys.* **103** 24

[18] Wang G Z, Geng B Y, Huang X M, Wang Y W, Li G H and Zhang L D 2003 *Appl. Phys. A – Mater.* **77** 933

[19] Tsuji I, Kato H, Kobayashi H and Kudo A 2004 *J. Am. Chem. Soc.* **126** 13406

[20] Kumar S S, Khadar M A, Nair K G M, Dhara S and Magudapathy P 2008 *J. Raman Spectrosc.* **39** 1900

[21] Dhara S, Arora A K, Bera S and Ghatak J 2010 *J. Raman Spectrosc.* **41** 1102

[22] Scocioreanu M, Baibarac M, Baltog I, Pasuk I and Velula T 2012 *J. Solid State Chem.* **186** 217

[23] Radhu S and Vijayan C 2011 *Mater. Chem. And Phys.* **129** 1132

[24] Cheng C, Xu G, Zhang H, Cao J, Jiao P and Wang X 2006 *Mater. Lett.* **60** 3561

[25] Wang X, Shi J, Feng Z, Li M and Li C 2011 *Phys. Chem. Chem. Phys.* **13** 4715

[26] Georgekutty R, Seery M K, and Pillai S C 2008 . *J. Phys. Chem. C* **112** 13563

[27] Banhemann D 2004 *Solar Energy* **77** 445

[28] Kryshtab T, Palacious Gomez J and Marin M 2006 *Kristallogr. Suppl.* **23** 287

[29] Li Y, Chen G, Zhou C and Sun J 2009 *Chem. Commun.* **15** 2020

D. W Synnott, M. K. Seery, S. J. Hinder, J. Colreavy and S. C. Pillai, **_Nanotechnology_**, 24, **2013**, 045704

---

[30] Tsuji I, Kato H and Kudo A 2006 *Chem. Commun.* **18** 1969

[31] Murakoshi K, Hosokawa H, Tanaka N, Saito M, Wada Y, Sakata T, Sori H and Yanagida S 1998 *Chem. Commun.* **3** 321

[32] Guo T, Chen Y, Liu L, Cheng Y, Zhang X, Ma B and Wei M 2012 *Cryst. Res. Technol.* **47** 449

[33] Synnott D W, Seery M K, Hinder S J, Michlits G and Pillai S C 2013 *Appl. Catal. B.* **130** 106

[34] Seery M K, George R, Floris P and Pillai S C 2007 *J Photoch. Photobio. A* **189** 258

[35] Pelaez M, Nolan N T, Pillai S C, Seery M K, Falaras P, Kontos A G, Dunlop P S M, Hamilton J W J., Byrne J, O'Shea K, Entezari M H, Dionysiou D D, 2012 *Appl. Catal. B.*. **125**, 331

[36] Nolan N T, Seery M K, Hinder S J, Healy L F, Pillai S C , 2010 *J. Phys. Chem. C*, **114**, 13026.

Full Reference

D. W Synnott, M. K. Seery, S. J. Hinder, J. Colreavy and S. C. Pillai, **_Nanotechnology_**, 24, **2013**, 045704

Journal Website

http://iopscience.iop.org/0957-4484/24/4/045704/article

D. W Synnott, M. K. Seery, S. J. Hinder, J. Colreavy and S. C. Pillai, *Nanotechnology*, 24, **2013**, 045704